

PAPERS | FEBRUARY 01 2024

Periodic strings: A mechanical analogy to photonic and phononic crystals

R. S. Pitombo ; M. Vasconcellos; P. P. Abrantes ; Reinaldo de Melo e Souza ; G. M. Penello ; C. Farina 



Am. J. Phys. 92, 108–114 (2024)

<https://doi.org/10.1119/5.0094212>



View
Online



Export
Citation

CrossMark



AAPT
PHYSICS EDUCATION®

Special Topic:
Teaching about the environment,
sustainability, and climate change

Read Now



Periodic strings: A mechanical analogy to photonic and phononic crystals

R. S. Pitombo,^{1,a)} M. Vasconcellos,^{2,b)} P. P. Abrantes,^{3,c)} Reinaldo de Melo e Souza,^{2,d)} G. M. Penello,^{4,e)} and C. Farina^{4,f)}

¹*Instituto de Física Teórica, UNESP—Universidade Estadual Paulista, ICTP South American Institute for Fundamental Research, Rua Dr. Bento Teobaldo Ferraz 271, 01140-070, São Paulo, SP, Brazil*

²*Instituto de Física, Universidade Federal Fluminense, 24210-346, Rio de Janeiro, RJ, Brazil*

³*Departamento de Física, Universidade Federal de São Carlos, Rodovia Washington Luís, km 235-SP-310, 13565-905, São Carlos, SP, Brazil*

⁴*Instituto de Física, Universidade Federal do Rio de Janeiro, 21941-972, Rio de Janeiro, RJ, Brazil*

(Received 1 April 2022; accepted 26 September 2023)

We present a theoretical study of a periodic vibrating string composed of a finite sequence of string segments connected periodically, with each segment characterized by a constant linear mass density. The main purpose is to provide a model that can mimic the properties of photonic or phononic crystals. This system displays frequency intervals for which wave propagation is not allowed (frequency bandgaps), in close analogy to photonic and phononic crystals. We discuss the behavior of these bandgaps when varying physical parameters, such as the values of the linear mass densities, the oscillation frequency, and the number of string segments constituting the entire system. © 2024 Published under an exclusive license by American Association of Physics Teachers.

<https://doi.org/10.1119/5.0094212>

I. INTRODUCTION

First proposed in 1987 by Yablonovitch¹ and John,² a photonic crystal is an arrangement of different material media in such a way that the crystal's optical parameters, and hence dielectric constants, are periodic. Historically, however, the study of one-dimensional (1D) periodic structures dates back to 1887 with Lord Rayleigh,³ who analyzed an experiment performed by Stokes and showed that light shone on this 1D crystal has a large reflectivity over a well-defined narrow frequency range.

When the period of the optical parameters' spatial modulation is comparable to the wavelength of the light propagating through the material, photonic bandgaps appear, which correspond to frequency ranges in which light propagation is forbidden in certain directions.^{4–9} Photonic crystals are the electromagnetic analog of crystalline solids in which forbidden energy bandgaps appear.¹⁰ These bandgaps heavily depend on the spatial modulation pattern, leading to several strategies for manufacturing photonic crystals.^{11,12} For further study concerning other properties and numerical modeling of these materials as well as experimental details on their fabrication and characterization, see Refs. 4 and 8, and references therein.

Since they enable light manipulation, photonic crystals have attracted much research interest since their discovery. Because of their capacity to confine and control light at a given wavelength, such materials have allowed for a variety of technological applications beyond the field of optical physics, such as in optoelectronics,¹³ displays,¹⁴ sensors,¹⁵ solar cells,¹⁶ light-emitting diodes,¹⁷ optical fibers,¹⁸ and in the construction of high-efficiency reflectors.¹⁹ In nature, photonic crystals are also present from inorganic opals²⁰ to different organic structures in butterfly wing scales, beetle scales, and bird feathers.²¹

Similarly, the propagation of elastic or acoustic waves in periodic composite media also produces bandgaps, which gave rise to the concept of phononic crystals, initially proposed in 1992 by Sigalas and Economou²² and later in 1993

by Kushwaha *et al.*²³ Since then, such systems have been extensively studied, presenting different applications in engineering and applied physics, such as in vibration reduction²⁴ and noise control.²⁵ Recent reviews covering these periodic structures can be found in Refs. 26–28. Similar phenomenology can be found in semiconductor heterostructures, where each semiconductor layer can be thought of as a different propagation medium for the electronic wavefunction (see Ref. 29 and references therein). Throughout this paper, we will refer more to photonic crystals, but the analogies can also be applied to phononic crystals.

The investigation of optical and acoustic responses of periodic structures is an active area of research and involves techniques and concepts rarely discussed in standard undergraduate textbooks. Coaxial cables have widely been used to emulate 1D photonic crystals, both theoretically and experimentally.^{30–35} However, since bandgaps appear as a consequence of wave interference, they can be engineered in any media in which waves propagate. In this regard, we propose the study of a conceptually simpler 1D photonic (phononic) crystal analog: the periodic string, which requires only an introductory classical mechanics background. Such a configuration consists of a finite sequence of interconnected string segments, presenting periodically alternating linear mass densities, which play the role of dielectric permittivities (densities) in photonic (phononic) crystals. The analogy is made possible because the light (sound) velocity in a given material is a function of its permittivity (density), while the wave velocity in a string depends on its linear mass density. As in the context of photonic crystals, bandgaps appear as a consequence of periodicity-induced destructive interference at given frequencies. Formally, periodicity would require an infinite set of strings, which is naturally not possible. Nonetheless, we show that, for realistic values of linear mass densities for the strings, only a few are needed to observe the bandgaps. Therefore, this simple analog possibly allows students to study the properties of photonic and phononic crystals in an undergraduate physics laboratory. We highlight that although a possible experimental setup for the system is

provided here, its implementation may present some challenges. However, it is pedagogically more tangible to study bandgaps emerging from the interference of mechanical waves in a string rather than from more abstract electromagnetic waves in material media, even from a theoretical point of view.

II. METHODOLOGY

In this section, we introduce the transfer-matrix method to study periodic strings. In addition to being easy to implement numerically, this method is powerful for studying 1D wave propagation and is a convenient tool for dealing with stratified media. It allows for the exact computation of transmittance and reflectance in non-trivial configurations,^{36–39} including photonic crystals.^{31,40} For an introduction to the transfer matrix formalism in the contexts of photonics, plasmonics, and condensed matter systems, see Refs. 41–43.

A. Interface between two different media

The starting point is to understand how waves behave at the interface of two different media. In Fig. 1, we consider two semi-infinite strings attached to each other at the origin, whose linear mass densities are μ_1 and μ_2 . Denoting the vertical displacement of a generic point of the string at instant t and space coordinate x by $u(x, t)$ and assuming small slopes ($|\partial u/\partial x| \ll 1$), $u(x, t)$ obeys the following wave equation:

$$\frac{\partial^2 u(x, t)}{\partial x^2} - \frac{\mu(x)}{T} \frac{\partial^2 u(x, t)}{\partial t^2} = 0, \quad (1)$$

where the tension T will be considered as uniform throughout the string, and $\mu(x)$ is the linear mass density. We first assume that $\mu(x) = \mu_1$ for $x < 0$, and $\mu(x) = \mu_2$ for $x > 0$. Physical solutions must satisfy the boundary conditions⁴⁴

$$u_1(0^-, t) = u_2(0^+, t), \quad (2)$$

$$\frac{\partial u_1}{\partial x}(0^-, t) = \frac{\partial u_2}{\partial x}(0^+, t), \quad (3)$$

where the index 1 applies to $x < 0$ and the index 2 applies to $x > 0$.

To compute the transmittance and reflectance, we search for harmonic solutions of frequency ω for Eq. (1) restricted to the boundary conditions (2) and (3). These can be written as

$$u_1(x, t) = A_1 e^{i(k_1 x - \omega t)} + B_1 e^{-i(k_1 x + \omega t)} \quad (x < 0), \quad (4)$$

$$u_2(x, t) = A_2 e^{i(k_2 x - \omega t)} + B_2 e^{-i(k_2 x + \omega t)} \quad (x > 0), \quad (5)$$

where A_i and B_i ($i = 1, 2$) are coefficients to be determined. The wave equation requires that

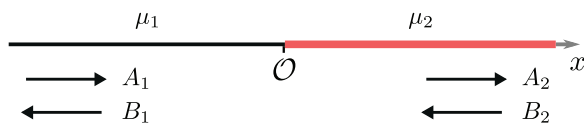


Fig. 1. Single string made out of two semi-infinite strings with different linear mass densities μ_1 and μ_2 .

$$k_j = \omega \sqrt{\frac{\mu_j}{T}} \quad \text{with } j = 1, 2, \quad (6)$$

and the boundary conditions give the following relations:

$$A_1 + B_1 = A_2 + B_2, \quad (7)$$

$$k_1(A_1 - B_1) = k_2(A_2 - B_2). \quad (8)$$

Defining $\eta = k_2/k_1$, this linear system of equations can be cast into the matrix form:

$$\begin{pmatrix} A_1 \\ B_1 \end{pmatrix} = \frac{1}{2} \begin{pmatrix} 1 + \eta & 1 - \eta \\ 1 - \eta & 1 + \eta \end{pmatrix} \begin{pmatrix} A_2 \\ B_2 \end{pmatrix} = \mathbb{T}_{1 \rightarrow 2} \begin{pmatrix} A_2 \\ B_2 \end{pmatrix}, \quad (9)$$

where $\mathbb{T}_{1 \rightarrow 2}$ is called the transfer matrix,⁴² and it relates the coefficients of the incoming wave to those of the outgoing wave at the interface. We can obtain the reflectance and transmittance directly from the transfer matrix elements, requiring no waves coming from the right ($B_2 = 0$). Note that when $\mu_2 > \mu_1$, that is, whenever the wave goes from a less refractive medium to a greater one, $1 - \eta < 0$, indicating that the reflected wave gains a phase of π .

Since the transmittance (reflectance) is the ratio between the transmitted (reflected) and incident powers, we can write

$$\mathcal{T} = \frac{k_2 |A_2|^2}{k_1 |A_1|^2} \quad \text{and} \quad \mathcal{R} = \frac{|B_1|^2}{|A_1|^2}. \quad (10)$$

Note that, since the wave velocity is different in each string, the transmittance is not just the square of the ratio between their amplitudes. From Eq. (9), we obtain $2A_1 = (1 + \eta)A_2$, implying

$$\mathcal{T} = \frac{4\eta}{(1 + \eta)^2}. \quad (11)$$

Equation (9) also yields

$$\mathcal{R} = \left(\frac{1 - \eta}{1 + \eta} \right)^2. \quad (12)$$

B. Finite string segment insertion

Let us now analyze the case where a finite string segment of length d and linear mass density μ_2 is inserted between two semi-infinite strings of equal linear mass densities μ_1 , as in Fig. 2. The transmittance and reflectance can be obtained through the total transfer matrix, relating the amplitudes of the solutions in the intervals $x < 0$ and $x > d$. The additional phase acquired by the propagation of the waves along the finite string segment can be taken into account by the propagation matrix

$$\mathbb{P}_2 = \begin{pmatrix} e^{-ik_2 d} & 0 \\ 0 & e^{ik_2 d} \end{pmatrix}, \quad (13)$$

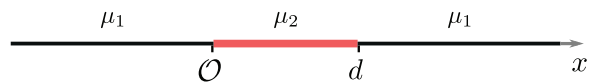


Fig. 2. Finite string segment with length d and linear mass density μ_2 placed between two semi-infinite strings of equal linear mass density μ_1 .

so that the total transfer matrix is

$$\mathbb{T}_{\text{tot}} = \overline{\mathbb{T}}_{1 \rightarrow 2} \mathbb{P}_2 \mathbb{T}_{2 \rightarrow 1}, \quad (14)$$

with $\mathbb{T}_{2 \rightarrow 1} = \overline{\mathbb{T}}_{1 \rightarrow 2}^{-1}$ by definition. From the total transfer matrix, the transmittance and reflectance are obtained in the same way as in the previous example, yielding

$$\mathcal{T} = \frac{k_f}{k_i} \frac{1}{|T_{11}^{\text{tot}}|^2}, \quad (15)$$

$$\mathcal{R} = \left| \frac{T_{21}^{\text{tot}}}{T_{11}^{\text{tot}}} \right|^2, \quad (16)$$

where k_i (k_f) stands for the wavenumber in the semi-infinite segment in the range $x < 0$ ($x > d$) and T_{ij}^{tot} ($i, j = 1, 2$) are the matrix elements of \mathbb{T}_{tot} . In the particular configuration of Fig. 2, the linear mass densities of the semi-infinite strings were chosen to be the same, and, consequently, $k_f/k_i = 1$. Explicit calculation (see the [Appendix](#)) results in

$$\mathcal{T} = \frac{1}{1 + \frac{(\mu_1^2 - \mu_2^2)^2}{\mu_1^2 \mu_2^2} \sin^2 \left(\omega d \sqrt{\frac{\mu_2}{T}} \right)}. \quad (17)$$

This expression is plotted in Fig. 3, in which we show the transmittance as a function of frequency, with $\mu_1 = 2$ g/m, $\mu_2 = 4\mu_1$, $d = 10$ cm, and $T = 1$ N. Note that the transmittance never vanishes and presents a periodic behavior with a period $\Delta\omega$ satisfying $\Delta k_2 d = \Delta\omega d \sqrt{\mu_2/T} = \pi$, where we used $k_2 = \omega \sqrt{\mu_2/T}$. Also, whenever $k_2 d = n\pi$ with n an integer, we have full transmittance. This was also expected from Eqs. (13) and (14) since, in this case, \mathbb{P}_2 and, consequently, \mathbb{T}_{tot} are ± 1 times the identity matrix. We invite the reader to explain these features from the interference of multiple reflections and check how time-saving the transfer matrix method is. Note that, in the limit $\mu_1 \rightarrow \infty$ for a fixed μ_2 , we have $\mathcal{T} \rightarrow 0$, except at the frequencies for which we have full transmittance. There is a close analogy between Eq. (17) and the transmission of electromagnetic waves propagating normally through a dielectric layer of finite thickness, the latter being obtained by substituting $\sqrt{\mu/T}$ in the former by the velocity of the light in the corresponding dielectric medium.

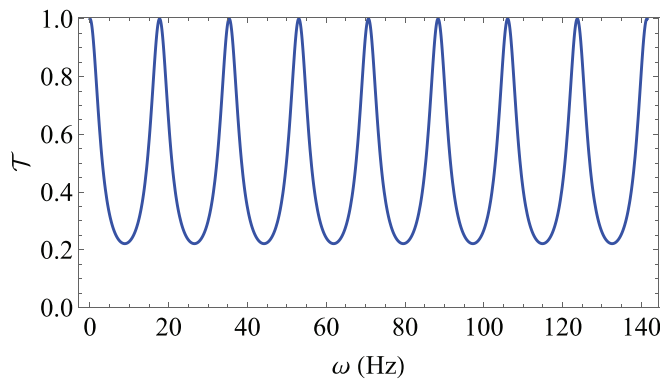


Fig. 3. Transmittance \mathcal{T} as a function of frequency ω for scattering by a single finite inserted segment. Here, $\mu_1 = 2$ g/m, $\mu_2 = 4\mu_1$, $d = 10$ cm, and $T = 1$ N.

C. Periodic string

Now, we reach the central purpose of this work: the study of a string containing N segments of linear mass density μ_2 interspersed with segments characterized by linear mass density μ_1 , as sketched in Fig. 4. Both types of segments are of length d . At both ends, a semi-infinite string of linear mass μ_1 is attached. By a straightforward generalization of the previous examples, the transfer matrix is now given by

$$\mathbb{T}_{\text{tot}} = \mathbb{T}_{1 \rightarrow 2} \left(\mathbb{P}_2 \mathbb{T}_{1 \rightarrow 2}^{-1} \mathbb{P}_1 \mathbb{T}_{1 \rightarrow 2} \right)^{N-1} \mathbb{P}_2 \mathbb{T}_{1 \rightarrow 2}^{-1}, \quad (18)$$

where \mathbb{P}_1 accounts for the propagation along segments of linear mass density μ_1 and is obtained from Eq. (13) by exchanging k_2 by k_1 . In Sec. III, we study Eq. (18) analytically, but it is instructive for students to gain some intuition by first analyzing some concrete examples, as we did in Subsections II A and II B.

III. RESULTS AND DISCUSSIONS

In this section, we analyze the transmittance of the periodic string described in Sec. II C. For this, we used the computational environment Mathematica, but no specific calculation techniques or any numerical approximations were needed. Throughout this section, we chose $d = 10$ cm and $T = 1$ N. In Fig. 5, we show the transmittance against the frequency for $\mu_1 = 2$ g/m and $\mu_2 = 4\mu_1$, which are typical values for paracord type IA and paracord type II. Each curve refers to a string with a given number N of inserted segments, the number of unit cells contained in the string. A striking feature in Figs. 5(b) and 5(c) is the presence of periodic frequency regions in which the transmittance goes to zero, revealing the presence of bandgaps. Note that we do not have bandgaps for $N = 2$ [Fig. 5(a)], although the transmittance is already much lower for some frequencies. As N increases, the transmission dips become more prominent, and bandgaps can be identified even for a modest value of $N = 7$ [Fig. 5(b)]. In addition, between these bandgaps, there is an oscillatory behavior of the transmittance, and the frequencies of these oscillations increase with N . We also see in the panels that the frequencies where we have the dips in the transmittance are essentially independent of N . Note that the dips roughly come in pairs. Physically, this is due to the fact that we have two different strings, setting up two natural frequency scales $\omega_j \sim 1/d \sqrt{T/\mu_j}$ ($j = 1, 2$). These features will be addressed in Sec. IV.

Figure 6 displays the transmittance against the density ratio μ_2/μ_1 of the string segments, with $\mu_1 = 2$ g/m and $N = 7$. The dashed gray line stresses that the outcome is full transmittance for $\mu_2/\mu_1 = 1$, as expected for a homogeneous medium. This plot indicates that, for a given frequency, we can always choose a density ratio value for which that frequency is contained in a bandgap. We see that the gaps get larger as the ratio μ_2/μ_1 increases, which is expected since

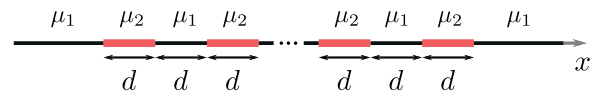


Fig. 4. The periodic string: A set of N segments with linear mass density μ_2 and size d alternating with segments of linear mass density μ_1 and of the same size.

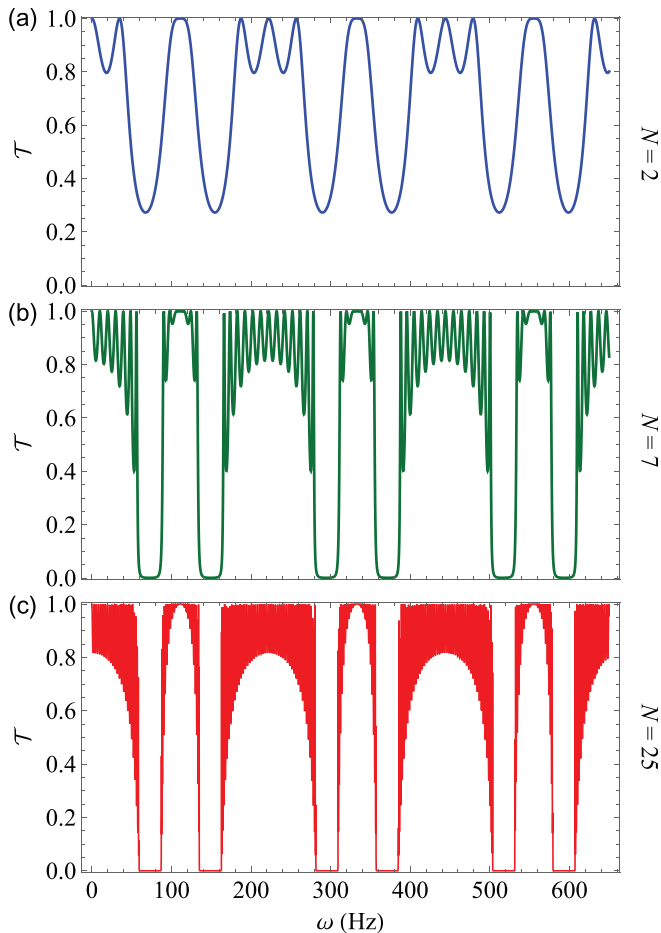


Fig. 5. Transmittance T as a function of the frequency ω for (a) $N=2$, (b) $N=7$, and (c) $N=25$. In all plots, we set $\mu_1 = 2$ g/m and $\mu_2 = 4\mu_1$.

the reflectivity in each segment increases in this case, as can be seen in Eq. (12).

In Fig. 7(a), we display the transmittance as a function of the wavenumbers of each string for $N=10$. Consider straight lines passing through the origin, with a constant slope given by the ratio $k_2/k_1 = \sqrt{\mu_2/\mu_1}$. For convenience, but without loss of generality, suppose that both μ_1 and μ_2 are fixed. In this case, the wavenumber of each string can only change through the frequency of the harmonic wave propagating along the string. Thus, starting at the origin and moving along any of these lines, we continuously increase the

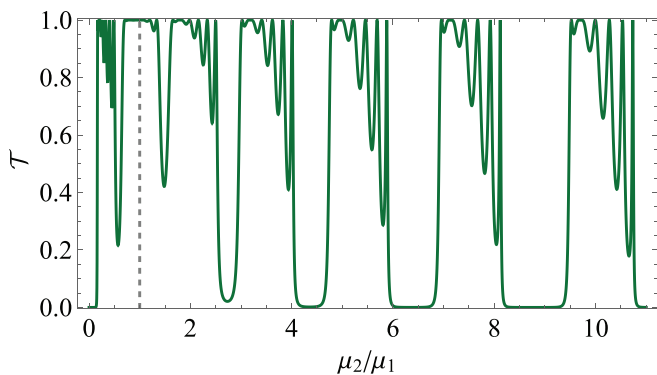


Fig. 6. Transmittance T as a function of the strings' density ratio μ_2/μ_1 for $N=7$, $\omega=500$ Hz, and $\mu_1 = 2$ g/m.

frequency of the wave. As it is evident from Fig. 7(a), the transmittance is always equal to 1 for $k_2/k_1 = 1$, as expected, since it implies $\mu_2 = \mu_1$. However, even for slight deviations of $k_2/k_1 = 1$, we necessarily pass through bandgaps when moving from the origin along a straight line. Note that the crossed bandgaps are very narrow for small deviations from unity. We can understand this result if we remember that there is no reflection of the incident wave for a homogeneous string. Nevertheless, as the ratio μ_2/μ_1 deviates from 1, the existence of the “lattice” (the periodic string arrangement) implies bandgaps start to appear. In this sense, this ratio measures the presence of the lattice and, consequently, how much scattering occurs in the system. Indeed, for $\mu_2/\mu_1 = 1$, we have $\eta = 1$ and we see that the transfer matrix given in Eq. (9) becomes the identity. It is worth noting that, even for slopes very different from the unity, besides wide bandgaps, we still have narrow ones, as shown in Fig. 5, which can be understood as similar cuts in Fig. 7 with constant slopes containing the origin. One could argue that there is a periodic pattern in Fig. 5, while this is not apparent for generic cuts in Fig. 7(a). Actually, as it will be described in Sec. IV, this periodicity only holds if the ratio k_1/k_2 is rational. This is true in Fig. 5 since $\mu_2 = 4\mu_1$ but this is not the case for lines crossing the origin with arbitrary slopes in Fig. 7(a).

Naively, one could think that Fig. 7(a) is symmetric with respect to the $k_1 = k_2$ line. However, this is not the case since our physical system is not symmetric under the exchange $k_2 \leftrightarrow k_1$ because the incident wave starts propagating through a semi-infinite string with linear mass density μ_1 and, after crossing the “periodic string,” is transmitted to another semi-infinite string with the same density μ_1 .

There are two interesting limiting cases. The first one is $k_2/k_1 \rightarrow \infty$, which can be thought of as taking $\mu_2 \rightarrow \infty$ and a finite value for μ_1 . Figure 7(b) shows the transmittance as a function of k_2 for $k_1 \sim 0$, and the outcome is zero transmittance for large k_2/k_1 , as expected since this limit corresponds to the string 2 behaving as a fixed wall (Dirichlet boundary condition). The second limiting case consists of $k_2 \ll k_1$, which corresponds to select $k_2 \sim 0$ in Fig. 7(a), resulting in Fig. 7(c). In this limit, we do not have transmission, except for increasingly narrower peaks around $2k_2d/\pi$ equal to an integer number. Physically, this happens because, in this case, we have constructive interference in all strings with linear mass density μ_2 .

IV. ANALYTICAL ORIGIN OF BANDGAPS

At this point, one might wonder why frequency gaps appear and if it is possible to determine their position analytically. Physically, bandgaps appear due to destructive interferences among the waves that are transmitted at each interface. Considering a small number of connections, like the setup depicted in Fig. 2, this analysis can be carried out without much calculation. We invite the reader to reobtain Eq. (17) from this reasoning. However, for a large number of strings, this procedure becomes complicated. Note that with only two connections, as shown in Fig. 2, we do not obtain gaps. Instead, we have frequencies that display dips in the transmittance. Strictly speaking, for any finite N , the transmittance is never zero, but, for large values of N , it is vanishingly small in some frequency ranges. As can be seen in Fig. 5, $N = 7$ is already a large value, given our chosen parameters, and bandgaps appear with virtually no transmitted

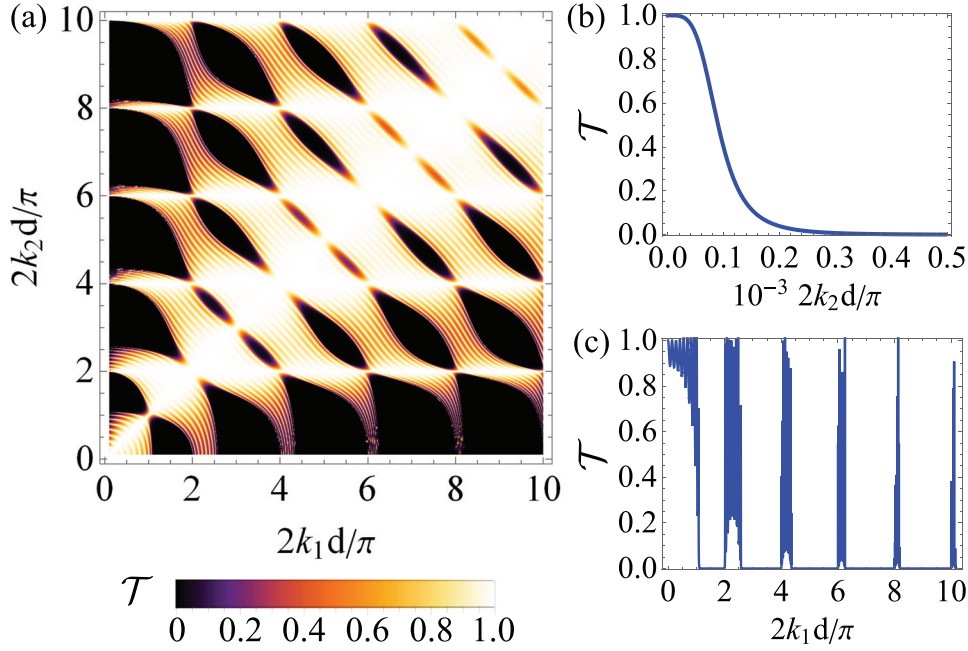


Fig. 7. Transmittance \mathcal{T} as a function of (a) k_1 and k_2 , (b) k_2 , for the slope $k_2 \gg k_1$, and (c) k_1 , for the slope $k_2 \ll k_1$. In all plots, $N = 10$.

wave. To be more precise, we may use the transfer matrix method. An analytical evaluation of Eq. (18) is possible thanks to periodicity and requires the $(N - 1)$ th power of the matrix $\mathbb{M} = \mathbb{P}_2 \mathbb{T}_{1 \rightarrow 2}^{-1} \mathbb{P}_1 \mathbb{T}_{1 \rightarrow 2}$. Since $\det \mathbb{M} = 1$, we have⁴⁵

$$\mathbb{M}^n = \begin{pmatrix} m_{11}U_{n-1}(a) - U_{n-2}(a) & m_{12}U_{n-1}(a) \\ m_{21}U_{n-1}(a) & m_{22}U_{n-1}(a) - U_{n-2}(a) \end{pmatrix}, \quad (19)$$

where m_{ij} denotes the matrix elements of \mathbb{M} , $a = (m_{11} + m_{22})/2$, and $U_n(x)$ are the Chebyshev polynomials of the second kind, given by

$$U_n(x) = \frac{\sin[(n+1)\cos^{-1}(x)]}{\sqrt{1-x^2}}. \quad (20)$$

Since $\cos^{-1}(x)$ is a purely imaginary number for $|x| > 1$ and recalling that $\sin(ix) = -i \sinh(x)$, we conclude that, for $|x| > 1$, $U_n(x)$ diverges exponentially for large n , leading to a divergence in all elements of \mathbb{T}_{tot} and, from Eq. (15), to a zero transmittance. The explicit calculation of a shows that the frequency bandgaps appear whenever the following condition is satisfied:

$$\frac{|(1 - \xi) \cos(k_- d) + (1 + \xi) \cos(k_+ d)|}{2} > 1, \quad (21)$$

with $k_{\pm} = k_2 \pm k_1$ and $\xi = (\mu_1 + \mu_2)/(2\sqrt{\mu_1\mu_2})$. Outside this range, $U_n(x)$ is an oscillating function, explaining the oscillations in the transmittance observed in Sec. III. In Fig. 8, we observe that the gaps appear exactly in the regions where $a > 1$.

Although we do not have an explicit solution of Eq. (21), its main properties can be readily grasped. First, note that, if $k_1 = k_2$ (homogeneous string), a will become

$\cos^2(2kd)$ and the condition (21) is never satisfied. Furthermore, when k_2 and k_1 are commensurable, a is a periodic function, and the bandgaps' locations and width will obey the same periodicity. For strings composed of appreciably different materials, that is, $2|\mu_1 - \mu_2|/(\mu_1 + \mu_2) \gtrsim 1$, we have $U_n \sim e^n$, and thus, from Eq. (16), $\mathcal{R} \sim e^{-n}$. This explains why bandgaps are perceptible even for small values of N in the previous section. Equation (21) allows us to interpret some of the results we obtained in Sec. III. There are two frequency scales involved in this expression, given by the conditions $k_{\pm}d = 2\pi$. In the particular case of Sec. III, we have $k_+ = 3k_-$, and thus, the function on the left-hand side of Eq. (21) is periodic, explaining the regular behavior displayed in Fig. 5. When we plot the transmittance as a function of μ_2/μ_1 , as in Fig. 6, we do not obtain periodic behavior. This is expected since the linear density, different from the frequency, does not depend linearly on the wavenumber.

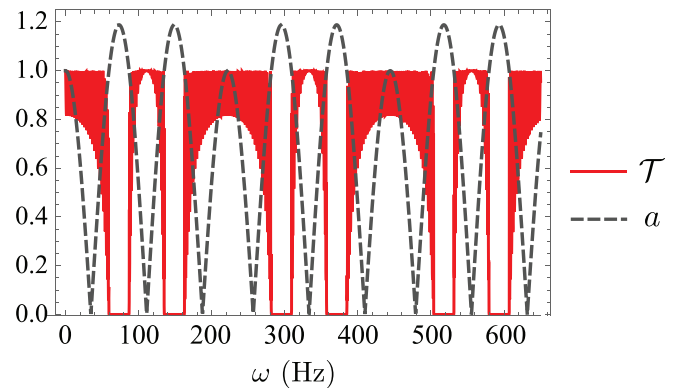


Fig. 8. Transmittance \mathcal{T} and the parameter a as a function of the frequency ω for $\mu_1 = 2 \text{ g/m}$, $\mu_2 = 4\mu_1$, and $N = 25$.

V. EXPERIMENTAL SETUP PROPOSAL

To experimentally probe the frequency intervals for which wave propagation is not allowed (the frequency bandgaps), an adaptation of Melde's original experiment⁴⁶ can be employed. In our experiment, Melde's single homogeneous string is replaced by a string made out of a periodic assembly of two string segments with different linear mass densities, as schematized in Fig. 4. In his original experiment, Melde was looking for stationary waves. In our case, since the main purpose is to observe bandgaps, we will focus on whether the wave can propagate to the end of the string. In other words, we will look for lack of oscillations in the segment furthest from the oscillator.

To assemble the experiment, we suggest using an electric vibrator, a signal generator to drive the vibrator, two strings with different linear mass densities (paracord type IA and paracord type II, for example), and hanging masses to control the tension.^{46,47} There are two different alternatives to observe the amplitude of the oscillations on the last segment of the string: the use of a camera with a ruler set behind the string or of stroboscopic light.⁴⁸

We suggest the use of paracords (or any nylon-based cord) due to their ability to melt when exposed to heat as one possibility to join two segments of different paracords seamlessly. We believe that this method could make the interface abrupt, respecting the boundary conditions used in the theoretical modeling. This procedure must be repeated to obtain the desired stratified medium with a specific number of segments. Considering seven repetitions to generate the situation of Fig. 5(b), and $d = 10$ cm, the total length of the interspersed ropes is 1.4 m. A 1.0 m paracord can then be used as the semi-infinite string at the end of the periodic assembly. As for the tension in the string, a hanging object of mass 100 g can be used to create a tension of about 1 N. Nevertheless, setting up this proposal might present some challenges. In particular, when joining the paracords through melting, some care should be taken not to alter the flexibility of the string. In addition, caution must also be taken to avoid the melted cord from shrinking and forming a knot with an extra mass, since this would not be in agreement with the boundary conditions employed in our theoretical model for the string. Controlling the length of the joined segments can also be challenging. A possible alternative to the melting procedure would be to create regions with greater linear mass density by using a single long cord and wrapping an extra cord around it.

As mentioned before, frequency bandgaps will correspond to frequencies with no oscillations, or zero transmission, in the last segment. Measurements of the wave amplitude in the last segment will be performed as a function of the electric vibrator frequency by using a camera (in the more expensive version of the experimental setup) or stroboscopic light. The use of a camera is straightforward, and analysis can be conducted by using the freeware Tracker (for an introduction to video analysis of experimental results using this freeware, we refer the reader to Ref. 49). For low-cost alternatives, a stroboscopic light can be employed, but only for visual observation, since it does not measure the amplitude of the oscillations on the last segment. The plot that relates the oscillation amplitude with frequency presents bandgaps for specific frequency ranges.

VI. FINAL REMARKS AND CONCLUSIONS

In this work, we employed the transfer matrix formalism to investigate wave propagation through a periodic string as an analog of photonic crystals. We determined the transmittance and discussed its dependence on the relevant physical parameters. The most remarkable result was the emergence of prohibited frequency bandgaps, even for low numbers of string segments. Ultimately, the system studied in this paper offers a variety of interesting aspects to explore, providing much physical intuition into quantum systems. We highlight that our results are an exact analog for one-dimensional photonic and phononic crystals, as we have explored throughout this paper. Therefore, the mechanical system we present here is an excellent route to get undergraduate students in touch with physical concepts rarely covered in standard textbooks. It can also arouse students' interest in other topics and motivate further studies, as the techniques we use have applications in different physical situations and can be generalized for more complex problems, as discussed throughout the text.

ACKNOWLEDGMENTS

R.S.P. and C.F. thank L. O. A. Azevedo for useful discussions. R.S.P. and P.P.A. acknowledge Fundação de Amparo à Pesquisa do Estado de São Paulo (FAPESP) (Grant Nos. 2022/05236-1 and 2021/04861-7) for financial support. M.V.S acknowledges Coordenação de Aperfeiçoamento de Pessoal de Nível Superior (CAPES) (Grant No. 88887.635842/2021-00) for financial support. G.P.M acknowledges Fundação de Amparo à Pesquisa do Estado do Rio de Janeiro (FAPERJ) (Nos. E-26/210.321/2022, E-26/210.019/2021, and E-26/010.001805/2019). C.F. acknowledges Conselho Nacional de Desenvolvimento Científico e Tecnológico (CNPq) (Grant No. 310365/2018-0). R.M.S. thanks the funding agencies.

AUTHOR DECLARATIONS

Conflict of Interest

The authors have no conflicts to disclose.

APPENDIX: EXPLICIT DERIVATION OF EQ. (17)

In this appendix, we obtain Eq. (17) employing the transfer matrix formalism and illustrating its convenience. It suffices to calculate the matrix element T_{11}^{tot} of the transfer matrix \mathbb{T}_{tot} , given by Eq. (14). We can write

$$\mathbb{T}_{\text{tot}} = \frac{1}{2} \begin{bmatrix} 1 + \eta & 1 - \eta \\ 1 - \eta & 1 + \eta \end{bmatrix} \begin{bmatrix} e^{ik_2d} & 0 \\ 0 & e^{-ik_2d} \end{bmatrix} \mathbb{T}_{1 \rightarrow 2}^{-1}. \quad (\text{A1})$$

Using that $\mathbb{T}_{1 \rightarrow 2}^{-1} = \mathbb{T}_{2 \rightarrow 1}$, the previous equation yields

$$\begin{aligned} T_{11}^{\text{tot}} &= \frac{1}{4} [e^{ik_2d}(1 + \eta)(1 + \eta^{-1}) + e^{-ik_2d}(1 - \eta)(1 - \eta^{-1})] \\ &= \frac{1}{4k_1k_2} [e^{ik_2d}(k_1 + k_2)^2 - e^{-ik_2d}(k_1 - k_2)^2]. \quad (\text{A2}) \end{aligned}$$

In going to the second line, we used the definition $\eta = k_2/k_1$ given in the main text. Consequently, using Eq. (15), the transmittance is obtained from

$$\frac{1}{T} = \frac{1}{16k_1^2 k_2^2} \left[(k_1 + k_2)^2 e^{-ik_2 d} - (k_1 - k_2)^2 e^{ik_2 d} \right] \times \left[(k_1 + k_2)^2 e^{ik_2 d} - (k_1 - k_2)^2 e^{-ik_2 d} \right]. \quad (\text{A3})$$

After lengthy but straightforward manipulations, we arrive at Eq. (17).

- ^{a)}Electronic mail: rs.pitombo@unesp.br, ORCID: 0000-0001-7573-1551.
- ^{b)}Electronic mail: mateusvsiqueira@gmail.com, ORCID: 0000-0001-6386-3530.
- ^{c)}Electronic mail: ppabrant91@gmail.com, ORCID: 0000-0002-6854-2223.
- ^{d)}Electronic mail: reinaldos@id.uff.br, ORCID: 0000-0002-6806-4567.
- ^{e)}Electronic mail: gpenello@if.ufrj.br, ORCID: 0000-0001-9067-6407.
- ^{f)}Electronic mail: farina@if.ufrj.br, ORCID: 0000-0002-0402-3723.
- ¹E. Yablonovitch, "Inhibited spontaneous emission in solid-state physics and electronics," *Phys. Rev. Lett.* **58**(20), 2059–2062 (1987).
- ²S. John, "Strong localization of photons in certain disordered dielectric superlattices," *Phys. Rev. Lett.* **58**(23), 2486–2489 (1987).
- ³L. Rayleigh, "XXVI. On the remarkable phenomenon of crystalline reflection described by Prof. Stokes," *London, Edinburgh, Dublin Philosoph. Mag. J. Sci.* **26**(160), 256–265 (1888).
- ⁴J. D. Joannopoulos, R. D. Meade, and J. N. Winn, *Photonic Crystals: Molding the Flow of Light* (Princeton U.P., Princeton, 1995), Chaps. 4 and 7.
- ⁵B. Schulkin, L. Sztancsik, and J. F. Federici, "Analytical solution for photonic band-gap crystals using Drude conductivity," *Am. J. Phys.* **72**(8), 1051–1054 (2004).
- ⁶F. Szmulowicz, "Analytic, graphical, and geometric solutions for photonic bandgaps," *Am. J. Phys.* **72**(11), 1392–1396 (2004).
- ⁷W. Guo, "Optical bandgaps as a result of destructive superposition of scattered waves," *Am. J. Phys.* **74**(7), 595–599 (2006).
- ⁸G. von Freymann, V. Kitaev, B. V. Lotsch, and G. A. Ozin, "Bottom-up assembly of photonic crystals," *Chem. Soc. Rev.* **42**(7), 2528–2554 (2013).
- ⁹A. Cerjan and S. Fan, "Complete photonic bandgaps in supercell photonic crystals," *Phys. Rev. A* **96**(5), 051802(R) (2017).
- ¹⁰N. W. Ashcroft and N. D. Mermin, *Solid State Physics* (Harcourt College Publishers, Orlando, 1976), Chap. 8.
- ¹¹S. H. Ryu, M. J. Gim, W. Lee, S. W. Choi, and D. K. Yoon, "Switchable photonic crystals using one-dimensional confined liquid crystals for photonic device application," *ACS Appl. Mater. Interfaces* **9**(3), 3186–3191 (2017).
- ¹²H. Wang, S. K. Gupta, B. Xie, and M. Lu, "Topological photonic crystals: A review," *Front. Optoelectron.* **13**(1), 50–72 (2020).
- ¹³J. Joannopoulos, P. Villeneuve, and S. Fan, "Photonic crystals: Putting a new twist on light," *Nature* **386**(6621), 143–149 (1997).
- ¹⁴A. C. Arsenault, D. P. Puzzo, I. Manners, and G. A. Ozin, "Photonic-crystal full-colour displays," *Nat. Photonics* **1**(8), 468–472 (2007).
- ¹⁵H. Xu, P. Wu, C. Zhu, A. Elbaz, and Z. Z. Gu, "Photonic crystal for gas sensing," *J. Mater. Chem. C* **1**(38), 6087–6098 (2013).
- ¹⁶P. Bermel, C. Luo, L. Zeng, L. C. Kimerling, and J. D. Joannopoulos, "Improving thin-film crystalline silicon solar cell efficiencies with photonic crystals," *Opt. Express* **15**(25), 16986–17000 (2007).
- ¹⁷E. Matioli, E. Rangel, M. Iza, B. Fleury, N. Pfaff, J. Speck, E. Hu, and C. Weisbuch, "High extraction efficiency light-emitting diodes based on embedded air-gap photonic-crystals," *Appl. Phys. Lett.* **96**(3), 031108 (2010).
- ¹⁸S. A. Cerqueira, Jr., "Recent progress and novel applications of photonic crystal fibers," *Rep. Prog. Phys.* **73**, 024401 (2010).
- ¹⁹A. Bruyant, G. Lérondel, P. J. Reece, and M. Gal, "All-silicon omnidirectional mirrors based on one-dimensional photonic crystals," *Appl. Phys. Lett.* **82**(19), 3227–3229 (2003).
- ²⁰C. I. Aguirre, E. Reguera, and A. Stein, "Tunable colors in opals and inverse opal photonic crystals," *Adv. Funct. Mater.* **20**(16), 2565–2578 (2010).
- ²¹K. L. Yu, T. X. Fan, S. Lou, and D. Zhang, "Biomimetic optical materials: Integration of nature's design for manipulation of light," *Prog. Mater. Sci.* **58**(6), 825–873 (2013).
- ²²M. M. Sigalas and E. N. Economou, "Elastic and acoustic wave band structure," *J. Sound Vib.* **158**(2), 377–382 (1992).
- ²³M. S. Kushwaha, P. Halevi, L. Dobrzynski, and B. Djafari-Rouhani, "Acoustic band structure of periodic elastic composites," *Phys. Rev. Lett.* **71**(13), 2022–2025 (1993).
- ²⁴D. Richards and D. J. Pines, "Passive reduction of gear mesh vibration using a periodic drive shaft," *J. Sound Vib.* **264**(2), 317–342 (2003).
- ²⁵José Sánchez-Dehesa, Victor M. Garcia-Chocano, Daniel Torrent, Francisco Cervera, Suitberto Cabrera, and Francisco Simon, "Noise control by sonic crystal barriers made of recycled materials," *J. Acoust. Soc. Am.* **129**(3), 1173–1183 (2011).
- ²⁶M. I. Hussein, M. J. Leamy, and M. Ruzzene, "Dynamics of phononic materials and structures: Historical origins, recent progress, and future outlook," *Appl. Mech. Rev.* **66**, 040802 (2014).
- ²⁷Y. F. Wang, Y. Z. Wang, B. Wu, W. Chen, and Y. S. Wang, "Tunable and active phononic crystals and metamaterials," *Appl. Mech. Rev.* **72**, 040801 (2020).
- ²⁸J. Liu, H. Guo, and T. Wang, "A review of acoustic metamaterials and phononic crystals," *Crystals* **10**(4), 305 (2020).
- ²⁹Germano M. Penello, "Progress in symmetric and asymmetric superlattice quantum well infrared photodetectors," *Ann. Phys.* **531**, 1800462 (2019).
- ³⁰A. Haché and L. Poirier, "Anomalous dispersion and superluminal group velocity in a coaxial photonic crystal: Theory and experiment," *Phys. Rev. E* **65**(3), 036608 (2002).
- ³¹M. M. Sánchez-López, J. A. Davis, and K. Crabtree, "Coaxial cable analogs of multilayer dielectric optical coatings," *Am. J. Phys.* **71**(12), 1314–1319 (2003).
- ³²A. Haché and A. Slimani, "A model coaxial photonic crystal for studying band structures, dispersion, field localization, and superluminal effects," *Am. J. Phys.* **72**(7), 916–921 (2004).
- ³³E. H. El Boudouti, Y. El Hassouani, B. Djafari-Rouhani, and H. Aynaou, "Two types of modes in finite size one-dimensional coaxial photonic crystals: General rules, and experimental evidence," *Phys. Rev. E* **76**(2), 026607 (2007).
- ³⁴E. H. El Boudouti, Y. El Hassouani, H. Aynaou, B. Djafari-Rouhani, A. Akjouj, and V. R. Velasco, "Electromagnetic wave propagation in quasi-periodic photonic circuits," *J. Phys.: Condens. Matter* **19**(24), 246217 (2007).
- ³⁵A. Perrier, Y. Guilloit, É. L. Cren, and Y. Dumeige, "A simple model system to study coupled photonic crystal microcavities," *Am. J. Phys.* **89**(5), 538–545 (2021).
- ³⁶J. S. Walker and J. Gathright, "Exploring one-dimensional quantum mechanics with transfer matrices," *Am. J. Phys.* **62**(5), 408–422 (1994).
- ³⁷R. B. Balili, "Transfer matrix method in nanophotonics," *Int. J. Mod. Phys. B*, 159–168 (2012).
- ³⁸T. Zhan, X. Shi, Y. Dai, X. Liu, and J. Zi, "Transfer matrix method for optics in graphene layers," *J. Phys.: Condens. Matter* **25**(21), 215301 (2013).
- ³⁹I. Haddouche and L. Cherbi, "Comparison of finite element and transfer matrix methods for numerical investigation of surface plasmon waveguides," *Opt. Commun.* **382**, 132–137 (2017).
- ⁴⁰J. Zi, J. Wan, and C. Zhang, "Large frequency range of negligible transmission in one-dimensional photonic quantum well structures," *Appl. Phys. Lett.* **73**(15), 2084–2086 (1998).
- ⁴¹P. Markoš and C. M. Soukoulis, *Wave Propagation: From Electrons to Photonic Crystals and Left-Handed Materials* (Princeton U.P., Princeton, 2008), Chap. 1.
- ⁴²P. A. D. Gonçalves and N. M. R. Peres, *An Introduction to Graphene Plasmonics* (World Scientific, Singapore, 2016), Sec. 2.4.
- ⁴³P. Pereyra, *Fundamentals of Quantum Physics: Textbook for Students of Science and Engineering* (Springer, Heidelberg, 2012), Sec. 4.1.
- ⁴⁴A. P. French, *Vibrations and Waves* (CRC Press, 2017), pp. 253–257.
- ⁴⁵M. Born and E. Wolf, *Principles of Optics: Electromagnetic Theory of Propagation, Interference, and Diffraction of Light* (Pergamon Press, New York, 1999), Subsection 1.6.5.
- ⁴⁶F. Melde, "Ueber die Erregung stehender Wellen eines fadenförmigen Körpers," *Ann. Phys. Chem.* **187**(12), 513–537 (1860).
- ⁴⁷G. Bozzo, F. de Sabata, S. Pistori, and F. Monti, "Imaging and studying standing waves with a homemade Melde-type apparatus and information and communication technology (ICT)," *Phys. Teach.* **57**(9), 612–615 (2019).
- ⁴⁸J. L. Le Carrou, D. Chadefaux, L. Seydoux, and B. Fabre, "A low-cost high-precision measurement method of string motion," *J. Sound Vib.* **333**(17), 3881–3888 (2014).
- ⁴⁹V. L. B. de Jesus, *Experiments and Video Analysis in Classical Mechanics* (Springer, Cham, 2017), p. 167.